the plant journal

SEB Society for Experimental Biology

The Plant Journal (2017) **91,** 251–262 doi: 10.1111/tpj.13560

Chlorosis caused by two recessively interacting genes reveals a role of RNA helicase in hybrid breakdown in *Arabidopsis thaliana*

Björn Plötner[1], Markus Nurmi[1], Axel Fischer[1], Mutsumi Watanabe[1], Korbinian Schneeberger[2], Svante Holm[3], Neha Vaid[1], Mark Aurel Schöttler[1], Dirk Walther[1], Rainer Hoefgen[1], Detlef Weigel[4] and Roosa A. E. Laitinen[1,*]

[1]*Max Planck Institute of Molecular Plant Physiology, Potsdam-Golm, Germany,*

[2]*Max Planck Institute for Plant Breeding, Cologne, Germany,*

[3]*Mid Sweden University, Sundsvall, Sweden, and*

[4]*Max Planck Institute for Developmental Biology, Tübingen, Germany*

Received 15 February 2017; revised 24 March 2017; accepted 30 March 2017; published online 4 April 2017.

*For correspondence (e-mail Laitinen@mpimp-golm.mpg.de).

SUMMARY

Hybrids often differ in fitness from their parents. They may be superior, translating into hybrid vigour or heterosis, but they may also be markedly inferior, because of hybrid weakness or incompatibility. The underlying genetic causes for the latter can often be traced back to genes that evolve rapidly because of sexual or host–pathogen conflicts. Hybrid weakness may manifest itself only in later generations, in a phenomenon called hybrid breakdown. We have characterized a case of hybrid breakdown among two *Arabidopsis thaliana* accessions, Shahdara (Sha, Tajikistan) and Lövvik-5 (Lov-5, Northern Sweden). In addition to chlorosis, a fraction of the F_2 plants have defects in leaf and embryo development, and reduced photosynthetic efficiency. Hybrid chlorosis is due to two major-effect loci, of which one, originating from Lov-5, appears to encode an RNA helicase (*AtRH18*). To examine the role of the chlorosis allele in the Lövvik area, in addition to eight accessions collected in 2009, we collected another 240 accessions from 15 collections sites, including Lövvik, from Northern Sweden in 2015. Genotyping revealed that Lövvik collection site is separated from the rest. Crosses between 109 accessions from this area and Sha revealed 85 cases of hybrid chlorosis, indicating that the chlorosis-causing allele is common in this area. These results suggest that hybrid breakdown alleles not only occur at rapidly evolving loci, but also at genes that code for conserved processes.

Keywords: chlorosis, hybrid breakdown, RNA helicase, *Arabidopsis thaliana*, local adaptation.

INTRODUCTION

Hybrids occasionally suffer from physiological and developmental problems, resulting in reduced fitness in comparison to their parents. These hybrid incompatibilities can impede gene flow in populations, and thus are important for genetic differentiation between populations and ultimately speciation in both plants and animals (Coyne and Orr, 2004). Hybrid difficulties often become obvious only in the F_2 or later generations, a phenomenon known as hybrid breakdown. Hybrid breakdown has been reported in many plants species including rice, wheat, rye, primrose and *Arabidopsis thaliana* (Sato and Morishima, 1988; Yamamoto *et al.*, 2007; Jiang *et al.*, 2008; Alcazar *et al.*, 2009; Bikard *et al.*, 2009). A theoretical model, proposed by William Bateson, Theodosius Dobzhansky and Hermann Muller, explains the evolution of hybrid breakdown. The model postulates that if independent mutations occur in two or more interacting genes and these later become fixed in two different populations, the newly evolved alleles can result in conflicts when brought together in a hybrid (Coyne and Orr, 2004). In hybrid breakdown, the conflict occurs when at least one of the interacting genes becomes homozygous in the F_2 or later generations.

Plant hybrid breakdown, like hybrid incompatibility in the F_1 generation, is often linked to growth defects, necrosis and chlorosis, which result in reduced viability and fertility (Bomblies and Weigel, 2007). Both hybrid necrosis and previously reported cases of hybrid chlorosis are linked to autoactivation of defence responses. While the former results in localized cell death, the latter is typified by reduced chlorophyll content and hence reduced

photosynthetic efficiency (Sato and Morishima, 1988; Tomar and Singh, 1998; Bomblies and Weigel, 2007; Ichitani *et al.*, 2012; Nakano *et al.*, 2015). *Arabidopsis thaliana* has been successfully used to unravel the genetic mechanisms of many cases of F_1 hybrid weakness (Bomblies and Weigel, 2007; Alcazar *et al.*, 2009; Chae *et al.*, 2014; Todesco *et al.*, 2014; Swiadek *et al.*, 2017). So far, only few genes or mechanisms underlying hybrid breakdown have been reported, but none of them was specifically shown for hybrid chlorosis (Alcazar *et al.*, 2009; Bikard *et al.*, 2009; Durand *et al.*, 2012). Therefore, investigation of genetic and phenotypic factors associated with hybrid chlorosis will improve our understanding of different origins of hybrid incompatibilities.

In addition to biotic and abiotic factors as causes, chlorosis can also arise due to a delay in chloroplast biogenesis, functionality or metabolism (Stern *et al.*, 2010). For example, the absence of enzymes involved in rRNA processing during ribosome biogenesis, including several members of DEAD-box RNA helicase family proteins, has been reported to result in a chlorotic phenotype in young leaves (Bollenbach *et al.*, 2005; Bang *et al.*, 2012; Chi *et al.*, 2012; Fristedt *et al.*, 2014). Additionally, loss of proteins involved in chloroplast RNA editing or essential for photosynthesis has been shown to result in slow greening of leaves (Zhou *et al.*, 2009; Stern *et al.*, 2010; Cao *et al.*, 2011; Chi *et al.*, 2012; Hu *et al.*, 2014). While several chlorotic mutants have been characterized in detail, factors involved in chlorosis in natural populations are not well known.

In this study, we investigate hybrid breakdown after a cross between the *A. thaliana* accessions Lövvik-5 (Lov-5) from Northern Sweden and Shahdara (Sha) from Tajikistan. Hybrid breakdown in the F_2 generation is accompanied by reduced chlorophyll content and photosynthetic efficiency in young leaves, decreased seed yield, and changes in early embryo and leaf development. Hybrid chlorosis was linked to two recessive interacting loci: one on chromosome 1 and one on chromosome 5. On chromosome 5, a gene encoding an uncharacterized DEAD-box RNA helicase 18 (*AtRH18*) was found to be necessary for hybrid chlorosis. The study provides novel insights into genetic, molecular and physiological architectures associated with hybrid breakdown in *A. thaliana*.

RESULTS

Hybrid breakdown between Sha and Lov-5 is associated with reduced chlorophyll content and photosynthetic efficiency

F_1 hybrids that were derived from reciprocal crosses between *A. thaliana* accessions Shahdara (Sha) from Tajikistan and Lövvik-5 (Lov-5) from Sweden did not differ from the parent phenotypes (Figure 1a and c), but about one-sixteenth of plants in F_2 populations had curled and chlorotic leaves (Figure 1a). The descendants of chlorotic F_2 plants no longer segregated this phenotype, indicating that two recessive loci that became homozygous in the F_2 are responsible for it. Chlorotic F_3 hybrid lines were used for further phenotypic and physiological analyses. We observed that 15.68% of the chlorotic F_3 hybrids had only a single or fused cotyledon (Figure 1b) with altered leaf vascular architecture. Despite the initial slower growth of the chlorotic leaves, their final rosette size was similar to that of the Lov-5 parent (Figure 1c). Nevertheless, the chlorotic F_3 hybrids produced significantly fewer seeds (Figure 1d) and they carried 14% of aborted seeds in their siliques (Figure 1e). This indicated that the chlorotic hybrids might have defects in embryo development. The height of the main stem, number of side shoots, rosette leaf number or flowering time did not differ between the chlorotic F_3 hybrids and the parents (Table S1). Next, we investigated the chlorophyll content of the three youngest leaves and mature leaves in parental lines and one chlorotic F_3 line (Figure 1f). In young leaves, the chlorotic F_3 hybrid contained significantly less chlorophyll in comparison to both parents, while the mature leaves that had stopped growing did not show a difference in the chlorophyll content (Figure 1f). Chlorotic plants also showed decreased starch content in young leaves (Figure 1g), most likely due to their reduced photosynthesis.

To determine if chlorosis was associated with altered photosynthetic efficiency, we performed chlorophyll-a fluorescence imaging measurements every second day across 2 weeks, starting 8 days after germination (DAG). The Fv/Fm ratio was used to investigate the maximum quantum efficiency of photosystem II across development in parents and in a chlorotic F_3 hybrid line. We found that only the young leaves, starting from leaf 4, of the chlorotic F_3 hybrids showed lower Fv/Fm ratios in comparison to the parents, while photosynthetic efficiency in fully grown leaves was similar in hybrids and parents (Figure 2a and b).

Because hybrid chlorosis can be a sign of activated defence against pathogens (Nakano *et al.*, 2015) and thus may be accompanied by necrosis, we stained young leaves of both parents and the F_3 hybrid with Trypan blue, which marks dead cells. We did not detect ectopic cell death (Figure S1a). Moreover, none of the several marker genes for defence response, namely, *PATHOGENESIS-RELATED GENE 1* (*PR1*), *PATHOGENESIS-RELATED GENE 5* (*PR5*), *PHOSPHOLIPASE D DELTA* (*PLDd*), *PLANT DEFENSIN 1.2* (*PDF1.2*) and *ENHANCED DISEASE SUSCEPTIBILITY 1* (*EDS1*), was induced in the chlorotic plants (Figure S1b), confirming that chlorosis was not due to activated defence responses. Grafting shoots from chlorotic F_3 plants to roots from either parent did not rescue chlorosis, indicating that the signal for chlorosis comes from the leaf tissues (Figure S2).

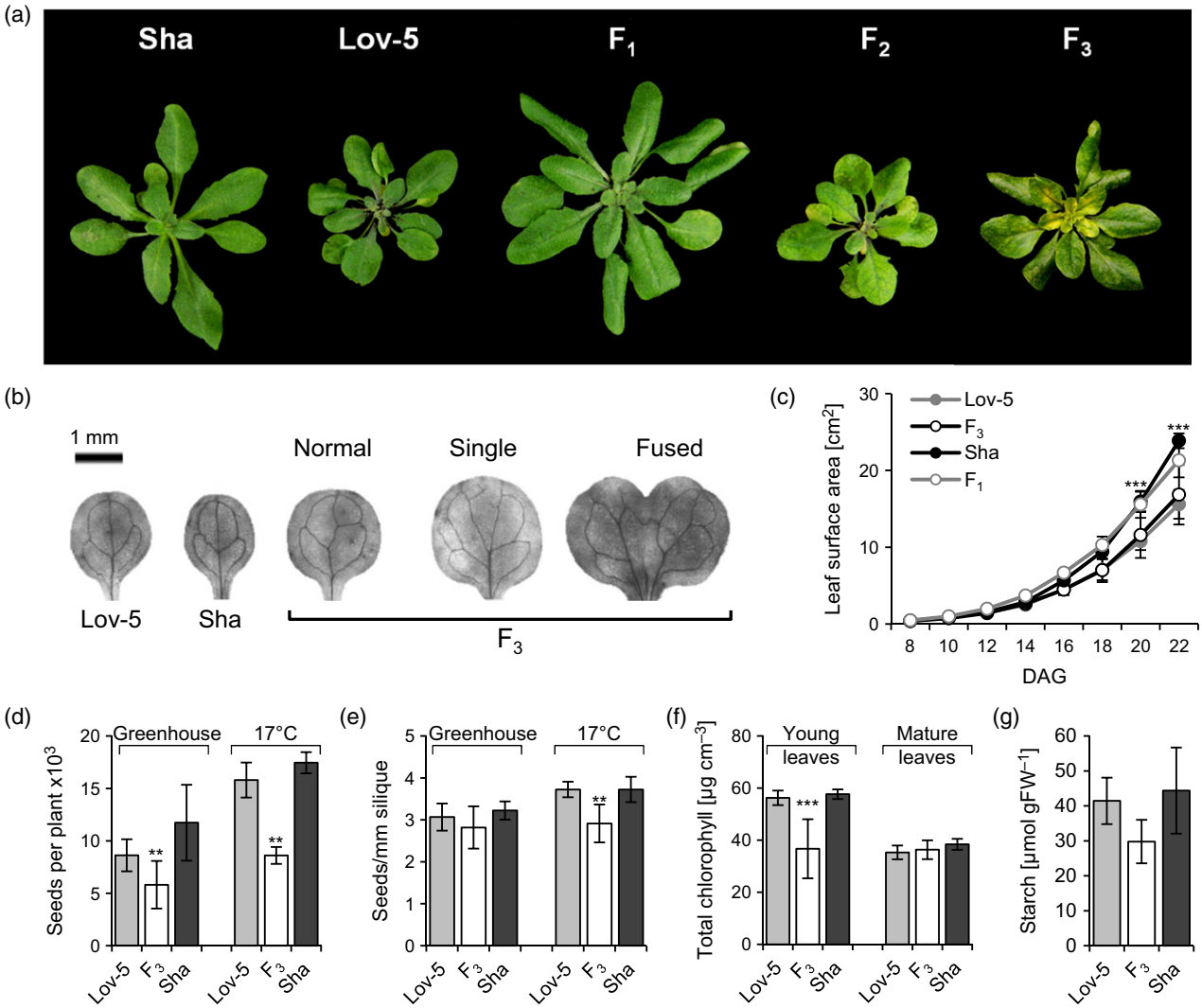

Figure 1. Characterization of hybrid breakdown in *Arabidopsis thaliana* accessions Shahdara (Sha) and Lövvik (Lov-5).
(a) Phenotype of 3-week-old Sha and Lov-5 plants, their F_1 progeny, and chlorotic F_2 and F_3 hybrids.
(b) Abnormal cotyledon phenotypes in F_3 plants fixed for the chlorosis alleles on chromosomes 1 and 5.
(c–g) Comparison of leaf surface area (c), seed number (d), seed index (e), chlorophyll content (f) and starch content (g) in hybrids and parents. In the greenhouse, the temperature was 21°C/19°C (day/night). For statistical significance a one-way ANOVA with Bonferroni's *post hoc* test for multiple comparisons was used with $*P < 0.05$, $**P < 0.01$ and $***P < 0.001$.

To further examine how hybrid chlorosis influences fitness in natural conditions, we grew chlorotic hybrids and parents outdoors on a field. Seeds were first sown in boxes in four replicates in early October 2012. After germination and growth for 3 weeks in the glasshouse, the boxes were transferred to the field throughout the winter. Phenotypes were scored in April 2013. In contrast to uniform greenhouse conditions, the chlorotic F_3 hybrids not only produced fewer seeds in the field (Figure 3c), but were also smaller than the parents (Figure 3a and b). In addition to fitness measurements, the field-grown plants were sampled for metabolic analysis in order to investigate if the leaf chlorosis was due to problems in uptake of nutrients. We compared levels of thiols, ions and amino acids in chlorotic hybrids and parents grown in the field and in the greenhouse. Hybrids accumulated more nitrate and ammonium as well as nitrogen-rich amino acids indicating problems in regulation of nitrogen metabolism both outdoors and in the greenhouse (Figure 4). Nevertheless, there was no indication of nutrient starvation in chlorotic hybrids. Taken together, we have shown that chlorosis starts in the fourth leaf of Lov-5 × Sha hybrids, resulting in initial reduction of photosynthetic efficiency and growth, from which the plants fully recover during maturation.

Two recessive genes underlie F_2 hybrid chlorosis

The segregation ratio of 1:15 (chlorotic:normal plants) in the F_2 generation suggested that alleles of two recessive

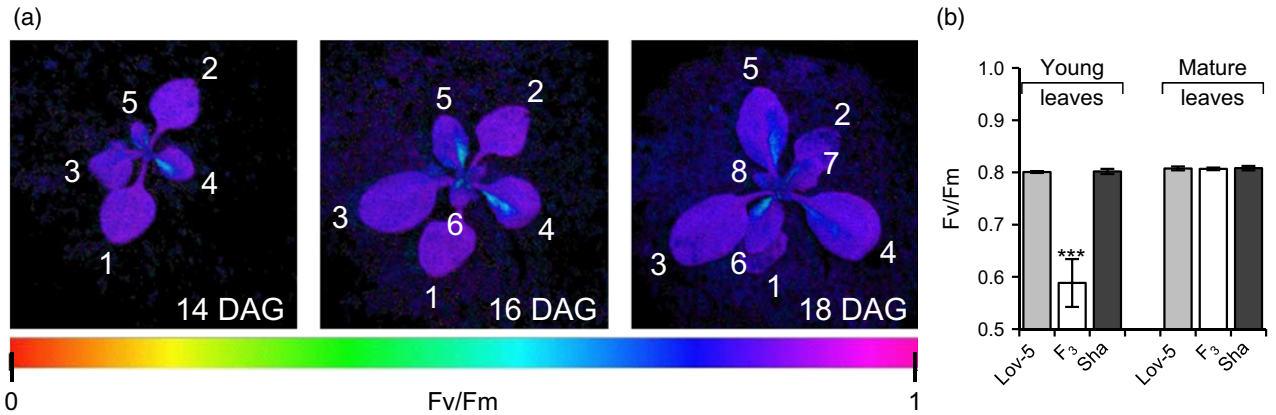

Figure 2. Investigation of photosynthetic efficiency of the leaves in chlorotic hybrids and parents.
(a) Chlorophyll-a fluorescence images showing the reduced maximum quantum efficiency of photosystem II (F_V/F_M) starting in leaf 4 at 14 days after germination (DAG).
(b) F_V/F_M in young and mature leaves. For statistical significance, a one-way ANOVA with Bonferroni's *post hoc* test for multiple comparisons was used with $*P < 0.05$, $**P < 0.01$ and $***P < 0.001$.

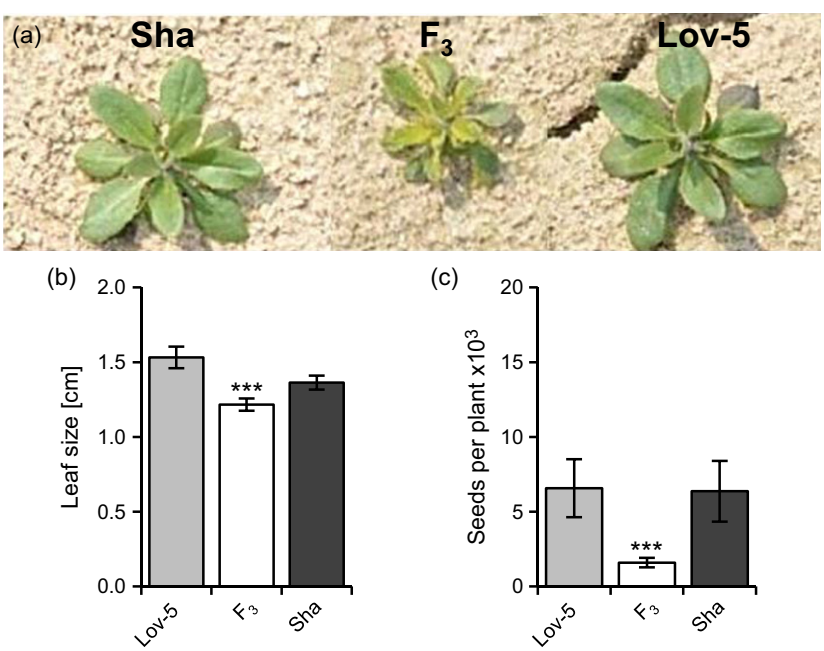

Figure 3. Phenotype of chlorotic hybrids and parents grown outdoors.
(a) F_3 hybrids show chlorosis, (b) the average length of the biggest leaf is reduced in F_3 hybrids in comparison to parents, and the F_3 hybrids produce less seeds than the parents (c). For statistical significance, a one-way ANOVA with Bonferroni's *post hoc* test for multiple comparisons was used with $*P < 0.05$, $**P < 0.01$ and $***P < 0.001$.

homozygous genes are causing the phenotype. The linkage to two loci, one on chromosome 1 contributed by Sha and one on chromosome 5 contributed by Lov-5, was directly demonstrated by whole-genome sequencing of a pool of 153 chlorotic F_2 plants (Figure 5). The final mapping interval on chromosome 1 contained 74 genes, while the chromosome 5 mapping interval contained 180 genes. By crossing Sha with 22 other accessions and Lov-5 with 13 other accessions, four additional cases (Lov-5 × Sij-1; Lov-5 × Sij-2; Lov-5 × Shigu-2; and Sha × Lov-1) of hybrid chlorosis were found (Figure S3a and b). Flanking markers for both intervals on chromosome 1 and chromosome 5 showed linkage to the same two loci in these other crosses as in Lov-5 × Sha, suggesting the same underlying genetic mechanism (Table S2).

A genome sequence comparison of the fully sequenced Arabidopsis accessions producing F_2 hybrid chlorosis when crossed with Lov-5 revealed that all accessions shared non-synonymous SNPs in 10 genes on chromosome 1 (www.1001genomes.org). However, none of the polymorphisms was specific for the chlorosis-producing accessions, suggesting that the underlying polymorphism is likely due to a larger structural variant that is not captured by Illumina re-sequencing. In order to further narrow

		Field						Greenhouse					
					Absolute value						Absolute value		
		Lov5	F3	Sha	Lov5	F3	Sha	Lov5	F3	Sha	Lov5	F3	Sha
Anion	Nitrate	a	b	a	1.88	6.24	0.48	a	a	b	29.1	38.4	9.0
nmol/mg FW	Sulfate	a	b	b	1.23	2.33	1.92	a	a	a	10.9	9.2	9.2
	Phosphate	a	b	a	0.21	0.31	0.21	a	a	a	5.0	6.2	4.2
	Chloride	a	a	a	1.84	2.06	2.20	ab	a	b	38.4	27.3	61.3
Cation	Ammonium	a	b	a	0.14	0.19	0.08	a	a	b	2.3	2.5	1.6
nmol/mg FW	Potassium	a	a	a	24.4	22.8	22.3	a	a	a	94.5	84.1	87.2
	Magnesium	a	a	a	3.1	2.9	2.4	a	a	a	8.3	8.4	7.1
	Calcium	a	a	a	12.5	13.5	9.2	a	a	a	6.5	8.4	5.7
Thiol	GSH	a	a	a	864.9	1030.5	698.4	a	ab	b	914.2	828.7	561.2
pmol/mg FW	gEC	a	a	a	9.5	8.4	7.8	a	a	a	9.4	8.2	6.8
	Cys	a	a	a	13.6	12.5	13.1	ab	a	b	24.4	28.2	21.4
Amino acid	Asn	a	b	a	466.6	1294.7	431.9	ab	a	b	1768.8	2507.7	933.7
pmol/mg FW	Arg	a	a	a	73.0	154.9	70.8	ab	a	b	1183.9	1728.1	132.6
	Gln	a	b	a	6482.0	12084.9	5412.1	ab	a	b	14370.3	17150.4	6455.6
	Thr	a	b	a	1036.7	1707.6	843.7	a	a	a	891.0	997.0	668.9
	Ala	a	b	a	1204.6	2167.6	1348.4	a	a	b	863.7	906.7	229.7
	Asp	a	b	a	3031.3	4462.1	3161.3	a	a	a	1657.9	2075.1	1356.3
	Ser	ab	a	b	2699.1	2939.2	1998.6	a	a	b	6483.4	6791.0	3359.6
	Lys	ab	a	b	50.8	59.5	46.5	a	ab	b	35.6	34.0	22.7
	Val	a	a	a	338.9	337.0	275.1	a	ab	b	176.9	139.6	81.6
	Leu	a	a	a	51.5	53.8	52.8	a	a	b	49.2	49.3	27.8
	Met	a	a	a	108.8	110.3	105.8	a	a	a	191.6	140.8	127.3
	Ile	a	a	a	69.5	68.0	63.0	ab	a	b	92.6	95.1	72.1
	Gly	a	a	a	5869.9	4025.7	2008.4	a	ab	b	6976.8	4292.5	1312.8
	Glu	a	a	a	6148.0	6442.3	6460.4	a	a	a	7427.6	7336.6	6487.4
	Trp	a	a	a	12.9	17.0	20.6	a	a	a	21.2	23.3	39.7
	Phe	a	a	a	164.6	156.2	154.9	a	a	a	212.7	138.8	140.2
	Tyr	a	a	a	48.5	44.2	43.4	a	a	a	23.7	20.5	18.6
	Cysth	a	ab	b	290.1	158.2	97.2	a	ab	b	247.2	164.6	62.4
	His	a	a	a	78.6	47.8	61.0	a	b	b	94.3	44.8	46.0

Figure 4. Heat map showing metabolites in hybrids in comparison to their parents in greenhouse and field-grown plants.
Heat map colours show the log2 fold differences for each metabolite relative to the metabolite levels averaged across all lines. The colour scale is given at the bottom. Data represent mean values of three biological samples. Different letters represent statistically significant differences ($P < 0.05$) using Tukey's test.

down the list of candidate genes from chromosome 1, we genotyped 288 F_3 plants, which were derived from a F_2 plant that was heterozygous in the interval on chromosome 1, with left (M08065) and right (M08460) border markers. From these, four of the non-chlorotic plants were homozygous Sha at M08460 and heterozygous at M08065, indicating recombination events in the mapping interval. By genotyping with additional markers in the mapping interval (M08350 and M08250), we were able to narrow down the list of candidates to seven genes (*At1g08030-At1g08210*; Tables 1 and S3). While artificial micro-RNAs (amiRNAs) against all seven genes in two chlorotic F_3 lines appeared to have some effect on the chlorosis phenotype, silencing of *At1g08140* and *At1g08210* rescued the

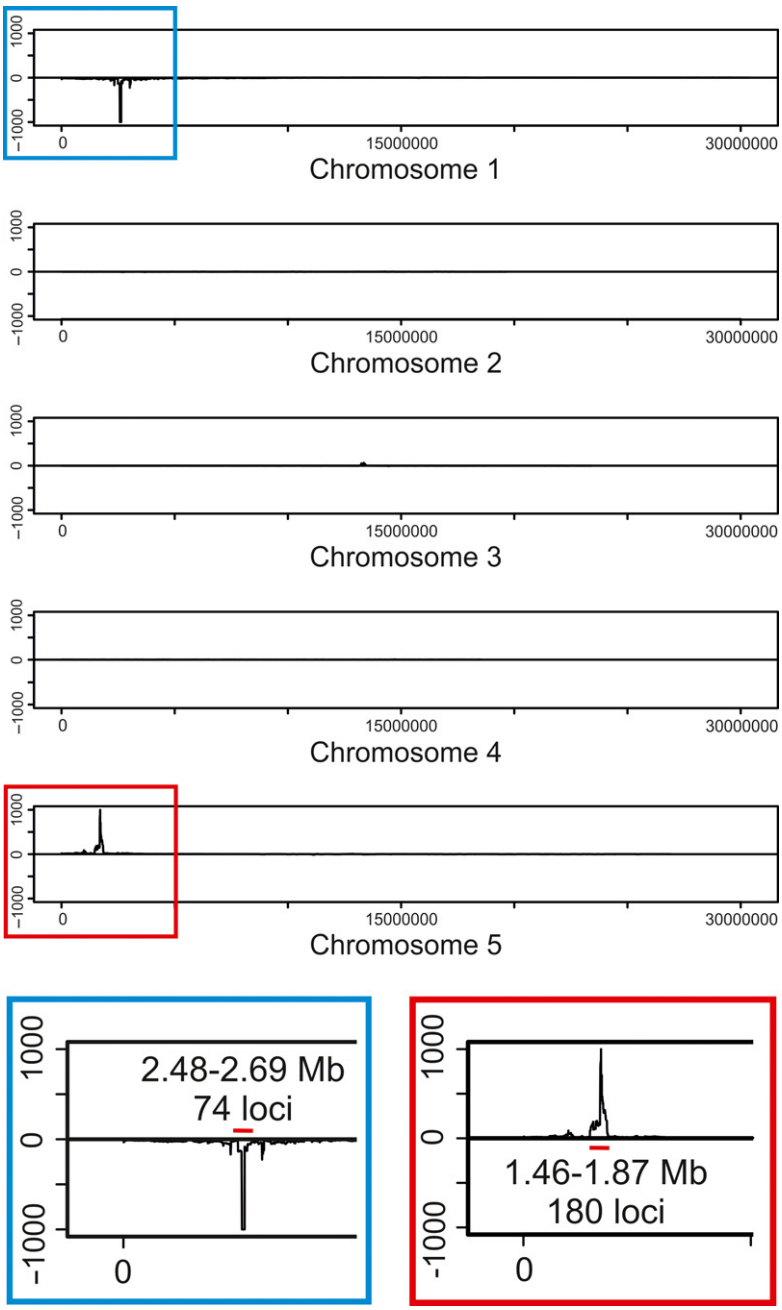

Figure 5. Illumina-based mapping of F_2 hybrid chlorosis.
A graph plotting the frequency of SNP calls in comparison to the reference sequence from the 153 chlorotic F_2 plants that were pooled and sequenced using Illumina sequencing. The high frequency of homozygous SNPs on chromosomes 1 and 5 revealed a linkage between these two loci. The analysis was done using SHORE mapping.

phenotype in nearly all transgenic lines, making these the most prominent candidates for the causal gene on chromosome 1 (Table S3). *At1g08140* encodes a protein of monovalent cation/hydrogen antiporter family (Sze *et al.*, 2004), Cation/H^+ exchanger 6A (CHX6a), which lies in a cluster with two other antiporters from the same family (*At1g08135*-CHX6b and *At1g08150*-CHX5). The second gene, *At1g08210*, encodes an uncharacterized pepsin-like aspartic protease family protein.

On chromosome 5, based on crosses and genome sequence comparisons among accessions, *At5g05450* was the most obvious candidate out of 26 genes with non-synonymous SNPs in comparison to Sha (Table 1). Two independent amiRNAs targeting *At5g05450*, which were confirmed to reduce the expression of the endogenous *At5g05450*, were able to fully rescue the chlorotic phenotype in several independent lines (Figure 6a and b; Table S3). *At5g05450* encodes a DEAD-box RNA helicase 18 (RH18) protein. Lov-5 *RH18* shows a unique polymorphism in its first exon (Serine 17 to Tyrosine; Figure 6d) in the Q-motif, which regulates substrate affinity as well as ATP binding and hydrolysis activity of

the helicase (Cordin *et al.*, 2006). The Lov-5 parent had significantly higher expression of *AtRH18* than Sha parent in young leaves and in seedlings, but the expression of *AtRH18* did not correlate with the chlorosis phenotype in the F_3 hybrid (Figure 6c). This indicates that chlorosis does not require reduced expression of *AtRH18*.

Table 1 List of candidate genes on chromosome 1 and chromosome 5

	Annotation
Chromosome 1	
AT1G08030	Tyrosylprotein sulphotransferase
AT1G08060	MORPHEUS MOLECULE 1 (MOM 1)
AT1G08065	Alpha carbonic anhydrase 5
AT1G08070	EMBRYO DEFECTIVE 3102 (EMB82)/ organelle transcript processing 82 (OTP 82)
AT1G08140	putative Na^+/H^+ antiporter
AT1G08150	putative Na^+/H^+ antiporter
AT1G08210	Eukaryotic aspartyl protease family protein
Chromosome 5	
AT5G05450	DEAD-box RNA helicase 18 (RH18)

DEAD-box RNA helicases are known to function in many aspects of RNA metabolism (Cordin *et al.*, 2006; Linder and Jankowsky, 2011). In *A. thaliana,* there are 56 different genes and two pseudogenes encoding DEAD-box RNA helicases (Boudet *et al.*, 2001; Mingam *et al.*, 2004). RH3, RH7, RH22 and RH39 are reported to be involved in chloroplast ribosome biogenesis, and the mutants display a chlorotic phenotype (Nishimura *et al.*, 2010; Chi *et al.*, 2012; Lee *et al.*, 2013). So far, *AtRH18* has not been functionally characterized. Of four different T-DNA insertion lines in the Col-0 reference background, two had insertions in exons (SALK_083512 and SAIL_34_A03) and homozygous mutants died as embryos (Figure 6e and f). Two other lines with insertions in their promoters (SALK_094004C and SALK_040682C) produced homozygous plants with chlorosis in young leaves (Figure 6e and g). This observation suggests that reduced activity of *At5g05450* in Col-0 leads to chlorosis.

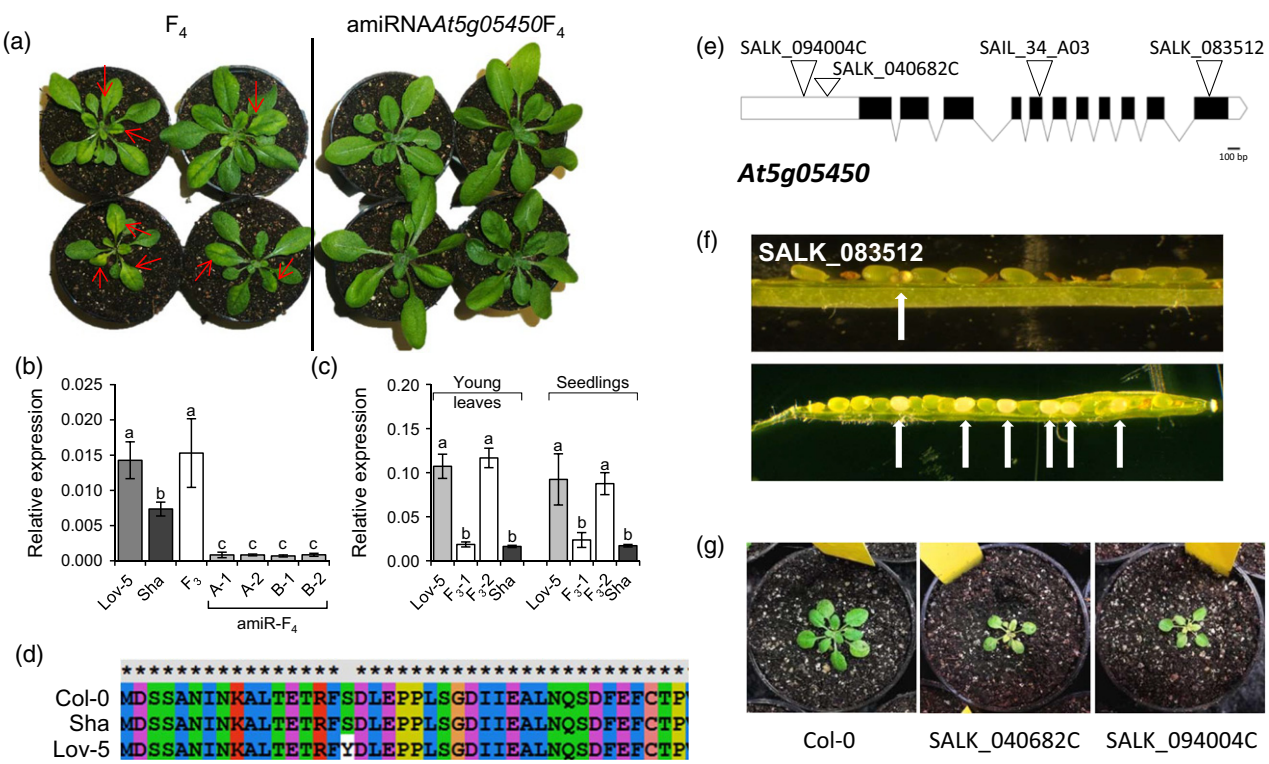

Figure 6. *At5g05450* encoding an RNA helicase (RH18) is necessary for hybrid chlorosis.
(a) Silencing *At5g05450* in the chlorotic F_3 lines using amiRNA suppresses the chlorotic phenotype in the F_4 lines. Red arrows point to chlorosis.
(b) Relative expression levels of the *At5g05450* in the parents, chlorotic F_3 line and four independent F_4 lines with the silenced *At5g05450* showing that amiR-*At5g05450* is functional and specific. A and B indicate two independent amiRNA constructs both targeting the *At5g05450* gene. Triplicates of two independent transformants were analysed.
(c) Expression of *At5g05450* in young leaves and seedlings of the parents and two chlorotic F_3 lines originating from different F_2 plants.
(d) Amino acid sequence comparison of the first exon of *At5g05450* showing the altering SNP in Lov-5 in comparison to Sha and Col-0.
(e) Schematic illustration of the exon-intron structure of the *At5g05450* illustrating the T-DNA insertion sites in mutants. Black boxes are exons.
(f) Opened siliques of *At5g05450* T-DNA line (SALK_083512). The white arrows point to seeds showing embryo lethality.
(g) Three-week old wild-type Col-0 and T-DNA mutants with insertion in the promoter of *At5g05450* showing leaf chlorosis in young leaves. For statistical significance, a one-way ANOVA with Bonferroni's *post hoc* test for multiple comparisons was used (mean ± SD).

Saccharomyces cerevisiae homolog of RH18, namely Spb4p, is involved in rRNA processing and ribosome biogenesis (de la Cruz *et al.*, 1998). So far, we have, however, not detected significant differences in the rRNA processing (cytosolic, chloroplastic and mitochondrial) in the chlorotic F_3 lines in comparison to the parents (Figure S4).

Hybrid chlorosis-causing alleles are commonly found in Northern Sweden

Based on the crosses (Figure S3), the chlorosis allele from Lov-5 seems to be rare in the global *A. thaliana* population. However, another accession from Lövvik (Lov-1) also showed chlorosis when crossed to Sha, suggesting that this allele may be common to the Lövvik area. To investigate this hypothesis, we collected 240 accessions from 15 different collection sites in the Lövvik-area in 2015 (Figure S5). We made crosses between the Sha parents and 84 of these individuals, and in addition eight individuals collected from eight different sites in 2009. Of these 109 individuals, 85 produced F_2 hybrid chlorosis in crosses with the Sha accession (Table S6). Among the plants collected in 2009, only the Eden and Ramsta individuals did not produce hybrid chlorosis when crossed to Sha. Of the 32 individuals from Lövvik in 2015, where we found the first hybrid chlorosis parent, 26 had the causal allele. Based on 2591 informative SNPs from RAD sequencing of the 240 accessions collected in 2015, we found that the individuals in different collection sites are genetically different; however, the individuals from the same population often cluster together (Figure S6). Interestingly, comparison of the mean similarities of the collection sites showed that the Lövvik was separated from the rest (Figure S7a and b). The heterozygosity among the Northern Sweden individuals was on average 1, 49% (ranging from 1, 30–1, 83%; Table S7), which is not particularly high but indicates that outcrossing occurs among the individuals in these sites.

DISCUSSION

We demonstrate that F_2 hybrid chlorosis, in a cross between the *A. thaliana* accessions Lov-5 and Sha, is due to alleles at two unlinked loci. The allele at the locus on chromosome 5 is locally common in Northern Sweden. We further show that a reduction in activity of the DEAD-box RNA helicase 18 (RH18) in Col-0 mutants leads to chlorosis, indicating that it is involved in causing chlorosis and consistent with the Lov-5 allele of the encoding gene, *At5g05450*, being causal for the F_2 hybrid chlorosis phenotype in the Sha $\times$ Lov-5 cross. DEAD-box RNA helicases are involved in several processes of RNA metabolism, such as RNA modification, RNA cleavage, RNA degradation, rRNA maturation, ribosome biogenesis and translation initiation, and therefore defects in RNA processing could be responsible for the observed phenotypes (Silverman *et al.*, 2003; Cordin *et al.*, 2006). Similar defects in early leaf development, including a reduction in cotyledon number as well as leaf curling, have been reported for several other RNA helicase mutants (Lange *et al.*, 2011; Liu *et al.*, 2016). RH18 had not been previously characterized, and we found that homozygous knockout mutants apparently die as embryos while the knockdown mutants show chlorosis in young leaves, a phenotype similar to that we observed in Lov-5 $\times$ Sha F_2 hybrids.

Other RNA helicases, including RH3, RH22 and RH39, are involved in chloroplast ribosome biogenesis and their perturbation is known to cause reduced chlorophyll content as well as pale coloration of the leaves. This supports the role of *RH18* in chlorosis; however, the function of RH18 in causing chlorosis in hybrids still remains to be investigated. In contrast to the mutants in Col-0 background, in which the reduced expression of *RH18* gene caused chlorosis, in Sha $\times$ Lov-5 hybrids, silencing of *RH18* using two independent amiRNA constructs rescued the phenotype of the chlorotic hybrids to mimic the phenotype of the parents. It is possible that the function of RH18 changes in different genetic backgrounds and that the epistatic interaction between the *RH18* and the yet unknown factor on chromosome 1 could influence the mode of action of RH18.

Whereas *RH18* on chromosome 5 was needed for chlorosis, on chromosome 1, based on further mapping efforts, crosses among accessions and sequence comparisons of candidate genes, two genes remained as most prominent candidates. The first gene, *At1g08140* encoding CHX6a, belongs to an antiporter family (Sze *et al.*, 2004), and the second candidate gene on chromosome 1, *At1g08210*, encodes a protein that belongs to the A1 family of pepsin-like aspartic proteases (Beers *et al.*, 2004). Members from this family have been shown to be involved in disease resistance (Xia *et al.*, 2004) and hybrid sterility (Chen *et al.*, 2008). In addition to these two genes, there were five other genes whose role in chlorosis cannot yet be ruled out. From these, *MORPHEUS MOLECULE 1* (*MOM1*) has a specific polymorphism among the 80 tested accessions in Sha resulting in a change of threonine to arginine. It has been speculated that the partial helicase motif in MOM1 could interact with another helicase (Amedeo *et al.*, 2000). It is intriguing to speculate that the polymorphism in *MOM1* could be involved in heterodimer formation with the Lov-5 allele of *RH18*. The future focus will be to investigate the causality of these candidates for hybrid chlorosis and further investigate the underlying mechanisms causing chlorosis together with *AtRH18*. Therefore, the involvement of *AtRH18* together with the second, yet unknown, causal gene provides new insights into the genetic architecture and mechanisms underlying F_2 hybrid breakdown.

Crosses among Sha parent and 109 individuals collected from Lövvik-are a showed that chlorosis-causing alleles were not specific for the Lövvik collection site but were

commonly occurring in this area. It is known that genes involved in hybrid breakdowns or incompatibilities are often thought to have evolved as a by-product of natural selection on genes underlying beneficial traits, such as pathogen resistance (Coyne and Orr, 2004). Further experiments are required to find out whether the chlorosis-causing allele of *RH18* has evolved through selection or drift. Several DEAD-box RNA helicases have been suggested to be involved in response to abiotic stresses (Owttrim, 2006; Vashisht and Tuteja, 2006) such as the barley DEAD-box RNA helicase, HVD1, which is transcriptionally induced by salt, cold and ABA (Nakamura *et al.*, 2004). Typical of the collected accessions is that they grow in south facing rocks and, different to many other Arabidopsis accessions, have almost no human disturbance. Furthermore, several studies have shown that Northern Swedish accessions are genetically different from Central European accessions (Nordborg *et al.*, 2005; François *et al.*, 2008; Horton *et al.*, 2012; Long *et al.*, 2013). They are more similar to accessions from Central Asia and Russia, which suggests that Arabidopsis have colonized Northern Sweden from these areas (Nordborg *et al.*, 2005). The first observation of the Arabidopsis in Northern Sweden where we collected is from 1984, while the oldest observation from the surrounding area was from 1857 (Mascher, 1990). This indicates that these populations are not recent and have had time to locally adapt to their growth habitats. This is supported by the study from Kerdaffrec *et al.* (2016), showing local adaptation in seed dormancy among *A. thaliana* populations from the same area. One possibility is that local adaptation in the Northern Sweden area involves changes in rRNA processing. Indeed, it was recently shown that Northern Swedish accessions have a high nuclear rDNA copy number compared with other global accessions (Long *et al.*, 2013). *RH18* was expressed more strongly in Lov-5 than in Sha, which could reflect the different function of RH18 in the parental variants. However, whether chlorosis-causing alleles have evolved from variation for adaptation to local environmental conditions or by genetic drift and how they cause hybrid chlorosis in combination with the chromosome 1 gene remains to be investigated in future.

EXPERIMENTAL PROCEDURES

Growth conditions of plants and physiological measurements

The Shahdara (Sha) and Lövvik-5 (Lov-5) cross was first reported in Salome *et al.* (2011). The global accessions were ordered from NASC, and all accessions used in this study are listed in Table S4. For the experiments, several independent F_3 lines originating from chlorotic F_2 plants were used. The T-DNA mutant lines SALK_083512, SAIL_34_A03, SALK_094004C and SALK_040682C were ordered from NASC. Seeds were stratified in 0.1% Agarose at 4°C in dark for 3–5 days, whereafter they were grown in growth chambers in LD (16 h day/8 h night) at 21°C and at 17°C with a light intensity of 150 μE (μmol m^{-2} sec^{-1}), or in the greenhouse at 21°C/19°C (day/night) temperature with varying light intensities. Northern Swedish accessions were vernalized for 10 weeks at 4°C to induce flowering. Total chlorophyll was extracted from leaves of five replicates with 80% (v/v) acetone (Arnon, 1949) and quantified spectrophotometrically according to Porra *et al.* (1989). Starch was extracted from the three youngest leaves according to Hendriks *et al.* (2003). Leaves were dark-adapted for 30 min prior to the chlorophyll-a fluorescence measurements with the Imaging-PAM M-Series (MAXI Version, Heinz Walz GmbH, Effeltrich, Germany). The minimal fluorescence in the dark-adapted stage, F_0, and maximal fluorescence during a saturating light pulse of 5000 μE m^{-2} sec^{-1}, F_M, were measured to calculate the maximum quantum efficiency of PSII using the formula $Fv/F_M = (F_M - F_0)/F_M$.

At least five replicates of Sha, Lov-5 and F_3 were used for all phenotypic measurements. Rosette diameter and leaf surface area were measured with ImageJ (http://rsbweb.nih.gov/ij) from photos taken every second day. For total seed yield, total weight of seeds was divided with the weight of 1000 seeds. The field trial was performed and seed yield was measured as described in Swiadek *et al.* (2017). Germination was counted 3 weeks after sowing and the survival of plants after winter in April 2013. The total leaf number was counted after bolting and the length of the biggest leaf was measured from photos of 10 randomly selected individuals of each box. Micrografting was done according to Thieme *et al.* (2015) with the following modifications; instead of 6-day-old seedlings, we used 10-day-old seedlings and after grafting they were grown for 14 days in SD (8 h day/16 h) at 22°C.

Mapping and genotyping

For mapping, 153 chlorotic F_2 plants were pooled, DNA was isolated using DNeasy Plant Mini Kit (Qiagen, Hilden, Germany) and sequenced using Illumina sequencing. Resequencing analysis of the bulked DNA and the parental genomes was performed with SHORE and GenomeMapper (Ossowski *et al.*, 2008; Schneeberger *et al.*, 2009a) following standard parameters. Allele frequency analysis was performed with an early version of SHOREmap (Schneeberger *et al.*, 2009b) by highlighting regions with fixed parental alleles assuming homozygous causal regions (Schneeberger, 2014). Markers used for further genotyping are listed in Table S5. RAD sequencing and the analysis of the Northern Swedish accessions were done similarly to Swiadek *et al.* (2017). Additionally, SNP- and samplewise novel allele to total coverage ratio were calculated to perform a Spearman correlation on the ratios of all SNPs covered with at least a 10 × coverage by all samples, and SNPs were showed polymorphism in at least one of the 241 accessions that were genotyped. Visualization was performed as heat map using heatmap.2 of the gplots R package. Heterozygosity was calculated for each sample from SNPs showing more than 10 × coverage.

amiRNA cloning

Artificial microRNAs (amiRNAs) were designed using the WMD3 online tool (http://wmd3.weigelworld.org) and cloned according to Schwab *et al.* (2006). The target sequences of each gene are listed in Table S3. Constructs were transformed to two chlorotic F_3 lines and then selected using BASTA. All constructs were introduced into *Agrobacterium tumefaciens* and plants were transformed by floral dip (Clough and Bent, 1998).

Metabolic profiling

Young leaves of at least five individuals from the field and from the greenhouse were sampled. Deep-frozen and powdered material

(20 mg for field-grown plants and 25 mg for greenhouse-grown plants) was homogenized in 300 μl methanol and then in 200 μl chloroform. The polar fraction was prepared by liquid partitioning into 400 μl of ultra-liquid chromatography/mass spectrometry (ULC/MS) water; 100-μl aliquots of polar fractions were vacuum-dried for metabolite profiles. One aliquot was dissolved in 500 μl of ULC/MS grade water for ion analysis. Free anions and cations were measured by Ion Chromatography System (Dionex ICS-3000, Sunnyvale, CA, USA) using the suppressed conductivity detection method according to the manufacturer's protocol (Dionex). Thiols were measured by a combination of monobromobimane fluorescent labelling and high-performance liquid chromatography (HPLC; Anderson, 1985; Fahey and Newton, 1987). Another vacuum-dried 100-μl aliquot was dissolved in 60 μl of 0.1 M HCl. A mixture of 20 μl of extract and 40 μl of 25 μM *N*-acetyl-cysteine as the internal standard was reacted with 3 μl of 30 mM tris (2-carboxyethyl) phosphine and 10 μl of 8.5 mM *N*-ethylmorpholine for 20 min at 37°C. After this reduction step, the reaction mix was reacted with 3 μl of 30 mM monobromobimane in acetonitrile for 20 min at 37°C in the dark. The labelling reaction was terminated by the addition of 10 μl of acetic acid, and the resulting solution was subjected to HPLC analysis as described previously (Hubberten *et al.*, 2012). Amino acids were measured by precolumn online derivatization with *O*-phthalaldehyde in combination with fluorescence detection (Lindroth and Mopper, 1979; Kim *et al.*, 1997). The last vacuum-dried 100-μl aliquot was dissolved in 60 μl of 0.1 M HCl. The 30 μl of extract was mixed in a HPLC vial with 30 μl of *O*-phthalaldehyde solution (Grom Analytik + HPLC GmbH, Herrenberg, Germany) diluted 10 times with water and 25 μl of borate buffer (1 M, pH 10.7) by autosampler, and the resulting solution was subjected to HPLC analysis as described previously (Hubberten *et al.*, 2012).

Real-time PCR

For the gene expression analysis, total RNA was isolated from young leaves using the InviTrap Spin Plant RNA Mini Kit (Stratec, Berlin, Germany) with three biological and two technical replicates. cDNA was synthetized using Maxima H minus Reverse Transcriptase (ThermoFisher Scientific, Waltham, USA) according to manufacturer's protocol. The primers for defense marker genes *PR1*, *PR5* and *PDF1.2* were designed according to Conn *et al.* (2008), and *UBIQ5* and *EF5* were used as housekeeping genes. For the expression analysis of *RH18,* two sets of primers (TCATGACCT GTGCTTCTGTTGAC/TGCCTTGTCTCTTGCATTCTGC and ACTGCC-CAAGGAAGAAGCCTATG/TGGCAGCTGAACGTATAATCGG) were designed using QuantPrime (Arvidsson *et al.*, 2008). *UBIQ10* and *EF1* were used as housekeeping genes.

rRNA analysis

Total RNA was extracted from at least three biological replicates each containing three young leaves using InviTrap Spin Plant RNA Mini Kit (Stratec, Berlin, Germany) as per manufacturer's instructions. For the rRNA quantification the Agilent 2100 bioanalyzer (Agilent Technologies, Santa Clara, CA, USA) was used. For the analysis of cytosolic rRNAs, primers for cDNA synthesis and reverse transcriptase polymerase chain reaction (RT-PCR) were designed as described by Liu *et al.* (2016), and circular RT-PCR was performed as described in Hang *et al.* (2014). RNA was ligated for 1 h at 37°C using T4 RNA ligase (New England Biolabs, Ipswich, USA). Reverse transcription using Maxima H Minus Reverse Transcriptase (ThermoFisher Scientific, Waltham, USA) was performed according to manufacturer's protocol. RNAase inhibitor (New England Biolabs, Ipswich, USA) was used to protect the samples. For the expression analysis of chloroplastic and mitochondrial rRNA, five biological and two technical replicates were used. Hexamer primers (ThermoFisher Scientific, Waltham, USA) were used for reverse transcription of RNA. For the analysis of chloroplastic rRNA, two sets of primers (GCTTTTTAAGTCCGCCGTCAA/TTGGTAGTTTCCACCGCCTGT for 16S and TGCTGCTGAATC-CATGGGCAGGCA/TGCTCCCATTTCGCTCGCCGCTACT for 23S) and for expression analysis of mitochondrial 18S rRNA one set of primers (AGCGAAACCCTCGTCTTGTGT/GCTCACTTCGGTTTT-CAAGCC) were used according to Piques *et al.* (2009). *UBIQ10* and *EF1* were used as reference genes.

ACKNOWLEDGEMENTS

Christa Lanz and Christian Jorzig are thanked for technical assistance. Hirofumi Ishihara is thanked for discussion on rRNA analysis. Karin Köhl and the Green Team of the Max Planck Institute of Molecular Plant Physiology are thanked for their assistance in taking care of plants. This work was supported by ERC AdG IMMUNEMESIS (D.W.) and the Max Planck Society (R.A.E.L.). The authors have no conflict of interest.

AUTHOR CONTRIBUTIONS

B.P. performed most of the experiments; M.N. performed rRNA experiments; A.F. analysed RAD sequencing data; M.W. performed metabolic experiments and data analysis; K.S. analysed the Illumina data; B.P., R.L. and S.H. collected seeds in Northern Sweden; N.V. contributed to the manuscript writing; M.A.S., R.H., D.Walther and D.Weigel supervised the experiments; R.A.E.L. conceived the original research plans and mapping, and supervised all experiments; R.A.E.L. and B.P. designed the experiments and wrote the article with D.Weigel; in addition, all authors contributed to the writing of the manuscript.

SUPPORTING INFORMATION

Additional Supporting Information may be found in the online version of this article.

Figure S1. Investigation of defence responses in chlorotic hybrids and parents.

Figure S2. Micrografting of the hybrid shoot to either Sha or Lov-5 parent or micrografting of the Sha or Lov-5 parental shoot to the hybrid root.

Figure S3. Identification of additional cases of hybrid chlorosis.

Figure S4. Analysis of the pre-rRNA processing in the hybrids and in the parents.

Figure S5. Map of sampling locations of Arabidopsis collected in Northern Sweden in 2015.

Figure S6. Genetic relationship of Arabidopsis collected in Northern Sweden in 2015.

Figure S7. Genetic relationship of different collection sites in Northern Sweden in 2015.

Table S1. Flowering traits of parents and chlorotic F_3 hybrid.

Table S2. Genotyping of chlorotic F_2 plants at markers on chromosomes 1 and 5.

Table S3. Candidate genes that were targeted with amiRNA on chromosomes 1 and 5 in chlorotic F_3 line.

Table S4. *Arabidopsis thaliana* accessions used in this study.

Table S5. List of genotyping markers on chromosomes 1 and 5.

Table S6. List of crosses done with Sha and the local Swedish accessions collected in 2009 and 2015.

Table S7. The percentage of heterozygosity in the Northern Swedish Arabidopsis collection sites.

REFERENCES

Alcazar, R., Garcia, A.V., Parker, J.E. and Reymond, M. (2009) Incremental steps toward incompatibility revealed by Arabidopsis epistatic interactions modulating salicylic acid pathway activation. *Proc. Natl Acad. Sci. USA*, **106**, 334–339.

Amedeo, P., Habu, Y., Afsar, K., Mittelsten Scheid, O. and Paszkowski, J. (2000) Disruption of the plant gene MOM releases transcriptional silencing of methylated genes. *Nature*, **405**, 203–206.

Anderson, M.E. (1985) Determination of glutathione and glutathione disulfide in biological samples. *Meth. Enzymol.* **113**, 548–555.

Arnon, D.I. (1949) Copper enzymes in isolated chloroplasts. *Polyphenoloxidase in Beta Vulgaris*. *Plant Physiol*, **24**, 1–15.

Arvidsson, S., Kwasniewski, M., Riano-Pachon, D.M. and Mueller-Roeber, B. (2008) QuantPrime – a flexible tool for reliable high-throughput primer design for quantitative PCR. *BMC Bioinform.* **9**, 465.

Bang, W.Y., Chen, J., Jeong, I.S. *et al.* (2012) Functional characterization of ObgC in ribosome biogenesis during chloroplast development. *Plant J.* **71**, 122–134.

Beers, E.P., Jones, A.M. and Dickerman, A.W. (2004) The S8 serine, C1A cysteine and A1 aspartic protease families in Arabidopsis. *Phytochemistry*, **65**, 43–58.

Bikard, D., Patel, D., Le Mette, C., Giorgi, V., Camilleri, C., Bennett, M.J. and Loudet, O. (2009) Divergent evolution of duplicate genes leads to genetic incompatibilities within *A-thaliana*. *Science*, **323**, 623–626.

Bollenbach, T.J., Lange, H., Gutierrez, R., Erhardt, M., Stern, D.B. and Gagliardi, D. (2005) RNR1, a 3′-5′ exoribonuclease belonging to the RNR superfamily, catalyzes 3′ maturation of chloroplast ribosomal RNAs in *Arabidopsis thaliana*. *Nucl. Acids Res.* **33**, 2751–2763.

Bomblies, K. and Weigel, D. (2007) Hybrid necrosis: autoimmunity as a potential gene-flow barrier in plant species. *Nat. Rev. Genet.* **8**, 382–393.

Boudet, N., Aubourg, S., Toffano-Nioche, C., Kreis, M. and Lecharny, A. (2001) Evolution of intron/exon structure of DEAD helicase family genes in Arabidopsis, Caenorhabditis, and Drosophila. *Genome Res.* **11**, 2101–2114.

Cao, Z.L., Yu, Q.B., Sun, Y., Lu, Y., Cui, Y.L. and Yang, Z.N. (2011) A point mutation in the pentatricopeptide repeat motif of the AtECB2 protein causes delayed chloroplast development. *J. Integr. Plant Biol.* **53**, 258–269.

Chae, E., Bomblies, K., Kim, S.T. *et al.* (2014) Species-wide genetic incompatibility analysis identifies immune genes as hot spots of deleterious epistasis. *Cell*, **159**, 1341–1351.

Chen, J., Ding, J., Ouyang, Y. *et al.* (2008) A triallelic system of S5 is a major regulator of the reproductive barrier and compatibility of indica-japonica hybrids in rice. *Proc. Natl Acad. Sci. USA*, **105**, 11436–11441.

Chi, W., He, B., Mao, J., Li, Q., Ma, J., Ji, D., Zou, M. and Zhang, L. (2012) The function of RH22, a DEAD RNA helicase, in the biogenesis of the 50S ribosomal subunits of Arabidopsis chloroplasts. *Plant Physiol.* **158**, 693–707.

Clough, S.J. and Bent, A.F. (1998) Floral dip: a simplified method for Agrobacterium-mediated transformation of *Arabidopsis thaliana*. *Plant J.* **16**, 735–743.

Conn, V.M., Walker, A.R. and Franco, C.M.M. (2008) Endophytic actinobacteria induce defense pathways in *Arabidopsis thaliana*. *Mol. Plant Microbe*, **21**, 208–218.

Cordin, O., Banroques, J., Tanner, N.K. and Linder, P. (2006) The DEAD-box protein family of RNA helicases. *Gene*, **367**, 17–37.

Coyne, J.A. and Orr, H.A. (2004) *Speciation*. Sunderland, MA, USA: Sinauer.

de la Cruz, J., Kressler, D., Rojo, M., Tollervey, D. and Linder, P. (1998) Spb4p, an essential putative RNA helicase, is required for a late step in the assembly of 60S ribosomal subunits in *Saccharomyces cerevisiae*. *RNA*, **4**, 1268–1281.

Durand, S., Bouche, N., Perez Strand, E., Loudet, O. and Camilleri, C. (2012) Rapid establishment of genetic incompatibility through natural epigenetic variation. *Curr. Biol.*, **22**, 326–331.

Fahey, R.C. and Newton, G.L. (1987) Determination of low-molecular-weight thiols using monobromobimane fluorescent labeling and high-performance liquid-chromatography. *Meth. Enzymol.* **143**, 85–96.

François, O., Blum, M.G.B., Jakobsson, M. and Rosenberg, N.A. (2008) Demographic history of European populations of *Arabidopsis thaliana*. *PLoS Genet.* **4**, 1–15.

Fristedt, R., Scharff, L.B., Clarke, C.A., Wang, Q., Lin, C., Merchant, S.S. and Bock, R. (2014) RBF1, a plant homolog of the bacterial ribosome-binding factor RbfA, acts in processing of the chloroplast 16S ribosomal RNA. *Plant Physiol.* **164**, 201–215.

Hang, R., Liu, C., Ahmad, A., Zhang, Y., Lu, F. and Cao, X. (2014) Arabidopsis protein arginine methyltransferase 3 is required for ribosome biogenesis by affecting precursor ribosomal RNA processing. *Proc. Natl Acad. Sci. USA*, **111**, 16190–16195.

Hendriks, J.H.M., Kolbe, A., Gibon, Y., Stitt, M. and Geigenberger, P. (2003) ADP-glucose pyrophosphorylase is activated by posttranslational redox-modification in response to light and to sugars in leaves of Arabidopsis and other plant species. *Plant Physiol.* **133**, 838–849.

Horton, M.W., Hancock, A.M., Huang, Y.S. *et al.* (2012) Genome-wide patterns of genetic variation in worldwide *Arabidopsis thaliana* accessions from the RegMap panel. *Nat. Genet.* **44**, 212–216.

Hu, Z., Xu, F., Guan, L., Qian, P., Liu, Y., Zhang, H., Huang, Y. and Hou, S. (2014) The tetratricopeptide repeat-containing protein slow green1 is required for chloroplast development in Arabidopsis. *J. Exp. Bot.* **65**, 1111–1123.

Hubberten, H.M., Klie, S., Caldana, C., Degenkolbe, T., Willmitzer, L. and Hoefgen, R. (2012) Additional role of O-acetylserine as a sulfur status-independent regulator during plant growth. *Plant J.* **70**, 666–677.

Ichitani, K., Takemoto, Y., Iiyama, K., Taura, S. and Sato, M. (2012) Chromosomal location of HCA1 and HCA2, hybrid chlorosis genes in rice. *Int. J. Plant Genomics* **2012**, 649081.

Jiang, W.Z., Chu, S.H., Piao, R.H., Chin, J.H., Jin, Y.M., Lee, J., Qiao, Y.L., Han, L., Piao, Z.Z. and Koh, H.J. (2008) Fine mapping and candidate gene analysis of hwh1 and hwh2, a set of complementary genes controlling hybrid breakdown in rice. *Theor. Appl. Genet.* **116**, 1117–1127.

Kerdaffrec, E., Filiault, D.L., Korte, A., Sasaki, E., Nizhynska, V., Seren, U. and Nordborg, M. (2016) Multiple alleles at a single locus control seed dormancy in Swedish Arabidopsis. *eLife*, **5**, 1–24. https://doi.org/10.7554/eLife.22502.

Kim, H.A., Hayashi, H., Chino, M. and Fujiwara, T. (1997) Analysis of O-acetyl-L-serine in in vitro cultured soybean cotyledons. In *Sulphur Metabolism in Higher Plants* (De Kok, I.S.L.J.D., Brunold, C. and Rennenberg, H., eds). Leiden: Backhuys, pp. 307–309.

Lange, H., Sement, F.M. and Gagliardi, D. (2011) MTR4, a putative RNA helicase and exosome co-factor, is required for proper rRNA biogenesis and development in *Arabidopsis thaliana*. *Plant J.*, **68**, 51–63.

Lee, K.H., Park, J., Williams, D.S., Xiong, Y., Hwang, I. and Kang, B.H. (2013) Defective chloroplast development inhibits maintenance of normal levels of abscisic acid in a mutant of the Arabidopsis RH3 DEAD-box protein during early post-germination growth. *Plant J.* **73**, 720–732.

Linder, P. and Jankowsky, E. (2011) From unwinding to clamping – the DEAD box RNA helicase family. *Nat. Rev. Mol. Cell Biol.* **12**, 505–516.

Lindroth, P. and Mopper, K. (1979) High-performance liquid-chromatographic determination of subpicomole amounts of amino-acids by precolumn fluorescence derivatization with ortho-phthaldialdehyde. *Anal. Chem.* **51**, 1667–1674.

Liu, Y., Tabata, D. and Imai, R. (2016) A cold-inducible DEAD-box RNA helicase from *Arabidopsis thaliana* regulates plant growth and development under low temperature. *PLoS ONE*, **11**, e0154040.

Long, Q., Rabanal, F.A., Meng, D. *et al.* (2013) Massive genomic variation and strong selection in *Arabidopsis thaliana* lines from Sweden. *Nat. Genet.* **45**, 884–890.

Mascher, J.W. (1990) Ångermanlands flora. In *Svensk Botanisk tidskrift*. Lund: Svenska botaniska föreningen.

Mingam, A., Toffano-Nioche, C., Brunaud, V., Boudet, N., Kreis, M. and Lecharny, A. (2004) DEAD-box RNA helicases in Arabidopsis thaliana: establishing a link between quantitative expression, gene structure and evolution of a family of genes. *Plant Biotechnol. J.* **2**, 401–415.

Nakamura, T., Muramoto, Y., Yokota, S., Ueda, A. and Takabe, T. (2004) Structural and transcriptional characterization of a salt-responsive gene encoding putative ATP-dependent RNA helicase in barley. *Plant Sci.* **167**, 63–70.

Nakano, H., Mizuno, N., Tosa, Y., Yoshida, K., Park, P. and Takumi, S. (2015) Accelerated senescence and enhanced disease resistance in hybrid chlorosis lines derived from interspecific crosses between tetraploid wheat and *Aegilops tauschii*. *PLoS ONE*, **10**, 1–26.

Nishimura, K., Ashida, H., Ogawa, T. and Yokota, A. (2010) A DEAD box protein is required for formation of a hidden break in Arabidopsis chloroplast 23S rRNA. *Plant J.* **63**, 766–777.

Nordborg, M., Hu, T.T., Ishino, Y. *et al.* (2005) The pattern of polymorphism in *Arabidopsis thaliana*. *PLoS Biol.* **3**, 1289–1299.

Ossowski, S., Schneeberger, K., Clark, R.M., Lanz, C., Warthmann, N. and Weigel, D. (2008) Sequencing of natural strains of *Arabidopsis thaliana* with short reads. *Genome Res.* **18**, 2024–2033.

Owttrim, G.W. (2006) RNA helicases and abiotic stress. *Nucl. Acids Res.*, **34**, 3220–3230.

Piques, M., Schulze, W.X., Hohne, M., Usadel, B., Gibon, Y., Rohwer, J. and Stitt, M. (2009) Ribosome and transcript copy numbers, polysome occupancy and enzyme dynamics in Arabidopsis. *Mol. Syst. Biol.* **5**, 1–17.

Porra, R.J., Thompson, W.A. and Kriedemann, P.E. (1989) Determination of accurate extinction coefficients and simultaneous-equations for assaying chlorophyll-a and chlorophyll-B extracted with 4 different solvents – verification of the concentration of chlorophyll standards by atomic-absorption spectroscopy. *Biochim. Biophys. Acta*, **975**, 384–394.

Salome, P.A., Bomblies, K., Laitinen, R.A.E., Yant, L., Mott, R. and Weigel, D. (2011) Genetic architecture of flowering-time variation in *Arabidopsis thaliana*. *Genetics*, **188**, U421–U313.

Sato, Y.I. and Morishima, H. (1988) Distribution of the genes causing F2 chlorosis in rice cultivars of the Indica and Japonica types. *Theor. Appl. Genet.* **75**, 723–727.

Schneeberger, K. (2014) Using next-generation sequencing to isolate mutant genes from forward genetic screens. *Nat. Rev. Genet.* **15**, 662–676.

Schneeberger, K., Hagmann, J., Ossowski, S., Warthmann, N., Gesing, S., Kohlbacher, O. and Weigel, D. (2009a) Simultaneous alignment of short reads against multiple genomes. *Genome Biol.* **10**, R98.

Schneeberger, K., Ossowski, S., Lanz, C., Juul, T., Petersen, A.H., Nielsen, K.L., Jorgensen, J.E., Weigel, D. and Andersen, S.U. (2009b) SHOREmap: simultaneous mapping and mutation identification by deep sequencing. *Nat. Meth.* **6**, 550–551.

Schwab, R., Ossowski, S., Riester, M., Warthmann, N. and Weigel, D. (2006) Highly specific gene silencing by artificial microRNAs in Arabidopsis. *Plant Cell*, **18**, 1121–1133.

Silverman, E., Edwalds-Gilbert, G. and Lin, R.J. (2003) DExD/H-box proteins and their partners: helping RNA helicases unwind. *Gene*, **312**, 1–16.

Stern, D.B., Goldschmidt-Clermont, M. and Hanson, M.R. (2010) Chloroplast RNA metabolism. *Annu. Rev. Plant Biol.* **61**, 125–155.

Swiadek, M., Proost, S., Sieh, D., Yu, J., Todesco, M., Jorzig, C., Rodriguez Cubillos, A.E., Plotner, B., Nikoloski, Z., Chae, E., Giavalisco, P., Fischer, A., Schroder, F., Kim, S.T., Weigel, D. and Laitinen, R.A. (2017) Novel allelic variants in ACD6 cause hybrid necrosis in local collection of Arabidopsis thaliana. *New Phytol.* **213**, 900–915.

Sze, H., Padmanaban, S., Cellier, F., Honys, D., Cheng, N.H., Bock, K.W., Conejero, G., Li, X.Y., Twell, D., Ward, J.M. and Hirschi, K.D. (2004) Expression patterns of a novel AtCHX gene family highlight potential roles in osmotic adjustment and K+ homeostasis in pollen development. *Plant Physiology*, **136**, 2532–2547.

Thieme, C.J., Rojas-Triana, M., Stecyk, E. *et al.* (2015) Endogenous Arabidopsis messenger RNAs transported to distant tissues. *Nat. Plants*, **1**, 15025.

Todesco, M., Kim, S.T., Chae, E., Bomblies, K., Zaidem, M., Smith, L.M., Weigel, D. and Laitinen, R.A.E. (2014) Activation of the *Arabidopsis thaliana* immune system by combinations of common ACD6 alleles. *PLoS Genet.* **10**, e1004459.

Tomar, S.M.S. and Singh, B. (1998) Hybrid chlorosis in wheat x rye crosses. *Euphytica*, **99**, 1–4.

Vashisht, A.A. and Tuteja, N. (2006) Stress responsive DEAD-box helicases: a new pathway to engineer plant stress tolerance. *J. Photoch. Photobio. B*, **84**, 150–160.

Xia, Y., Suzuki, H., Borevitz, J., Blount, J., Guo, Z., Patel, K., Dixon, R.A. and Lamb, C. (2004) An extracellular aspartic protease functions in Arabidopsis disease resistance signaling. *EMBO J.* **23**, 980–988.

Yamamoto, E., Takashi, T., Morinaka, Y., Lin, S., Kitano, H., Matsuoka, M. and Ashikari, M. (2007) Interaction of two recessive genes, hbd2 and hbd3, induces hybrid breakdown in rice. *Theor. Appl. Genet.* **115**, 187–194.

Zhou, W., Cheng, Y., Yap, A., Chateigner-Boutin, A.L., Delannoy, E., Hammani, K., Small, I. and Huang, J. (2009) The Arabidopsis gene YS1 encoding a DYW protein is required for editing of rpoB transcripts and the rapid development of chloroplasts during early growth. *Plant J.* **58**, 82–96.